



AST3100 Astrophysical transients

“You don’t observe the same Universe twice!”

Ziggy Pleunis
Meeting 1 Week 7
2022 October 27

 X-ray:
NASA/CXC/GSFC/
B.Williams et al;
Optical: DSS

First detection

OBSERVATIONS OF GAMMA-RAY BURSTS OF COSMIC ORIGIN

RAY W. KLEBESADEL, IAN B. STRONG, AND ROY A. OLSON

University of California, Los Alamos Scientific Laboratory, Los Alamos, New Mexico

Received 1973 March 16; revised 1973 April 2

ABSTRACT

Sixteen short bursts of photons in the energy range 0.2–1.5 MeV have been observed between 1969 July and 1972 July using widely separated spacecraft. Burst durations ranged from less than 0.1 s to ~ 30 s, and time-integrated flux densities from $\sim 10^{-5}$ ergs cm^{-2} to $\sim 2 \times 10^{-4}$ ergs cm^{-2} in the energy range given. Significant time structure within bursts was observed. Directional information eliminates the Earth and Sun as sources.

Subject headings: gamma rays — X-rays — variable stars

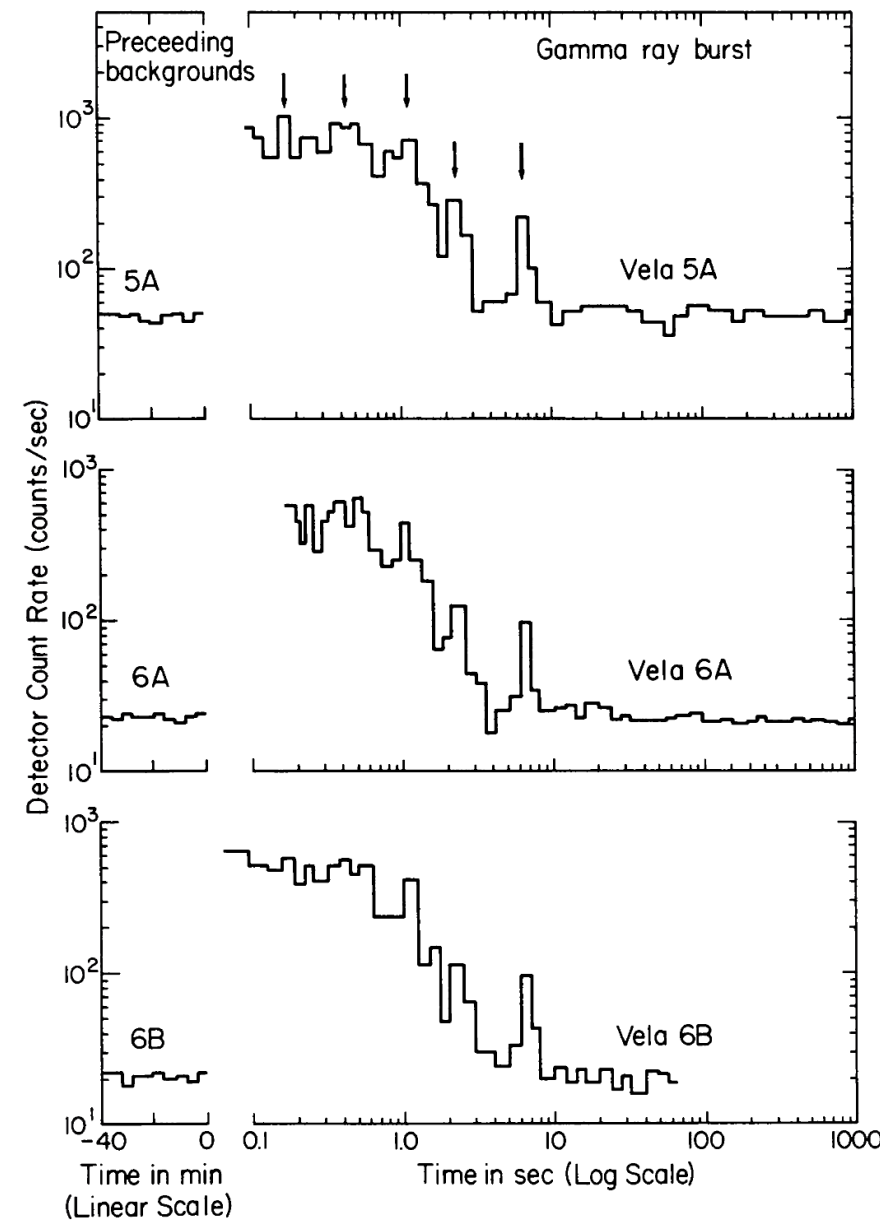


FIG. 1.—Count rate as a function of time for the gamma-ray burst of 1970 August 22 as recorded at three Vela spacecraft. Arrows indicate some of the common structure. Background count rates immediately preceding the burst are also shown. *Vela 5A* count rates have been reduced by 100 counts per second (a major fraction of the background) to emphasize structure.

Basic constraints

$$D \leq c \cdot \Delta t \approx 300 \text{ km.}$$

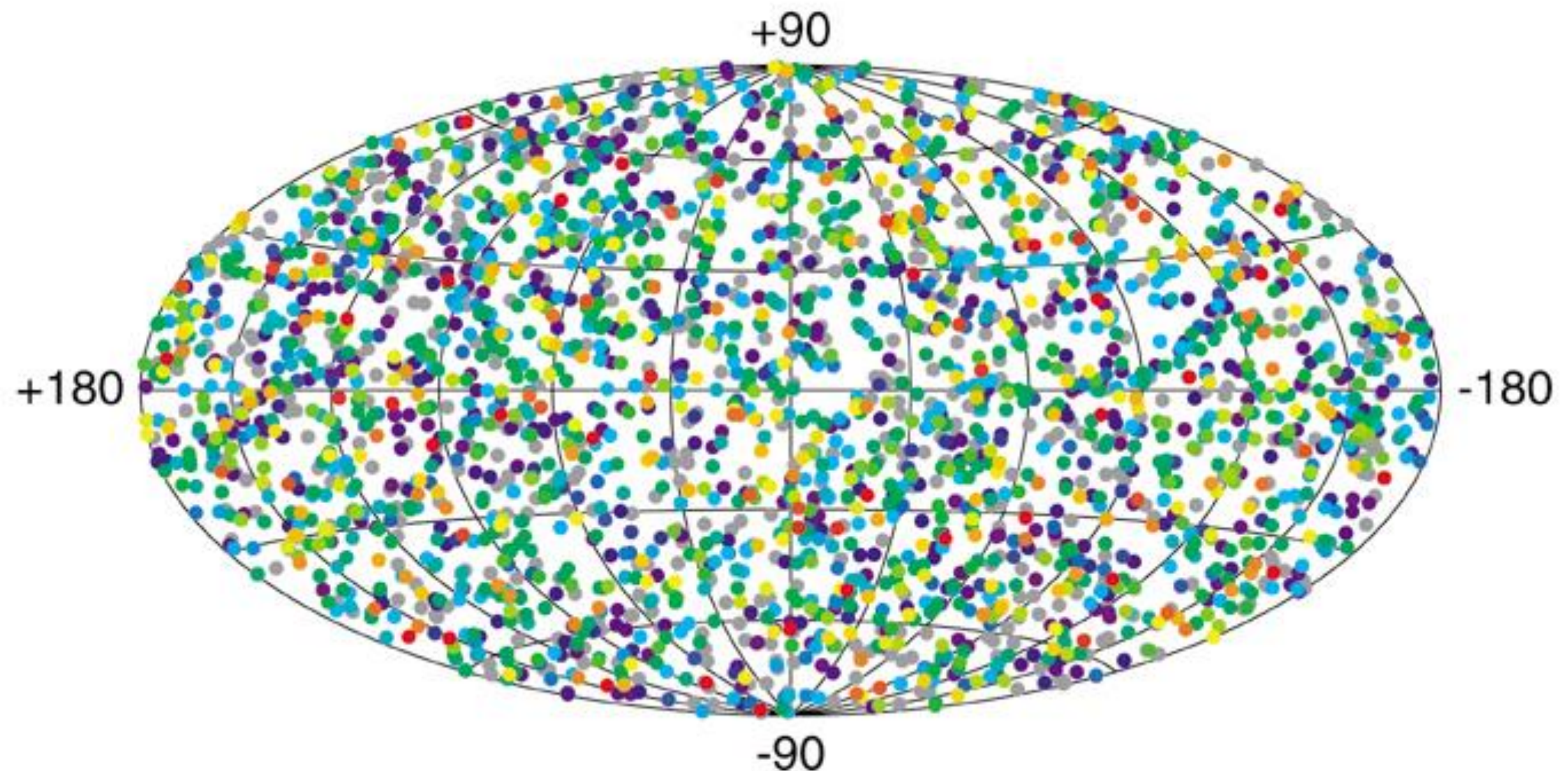
For $\Delta t \sim 1 \text{ ms}$

$$E_{\text{iso}} = 4\pi d^2 f \sim \begin{cases} 2 \cdot 10^{40} \text{ erg,} & \text{for } d = 15 \text{ kpc} \\ 2 \cdot 10^{41} \text{ erg,} & \text{for } d = 50 \text{ kpc} \\ 2 \cdot 10^{51} \text{ erg,} & \text{for } d = 5 \text{ Gpc} \end{cases}$$

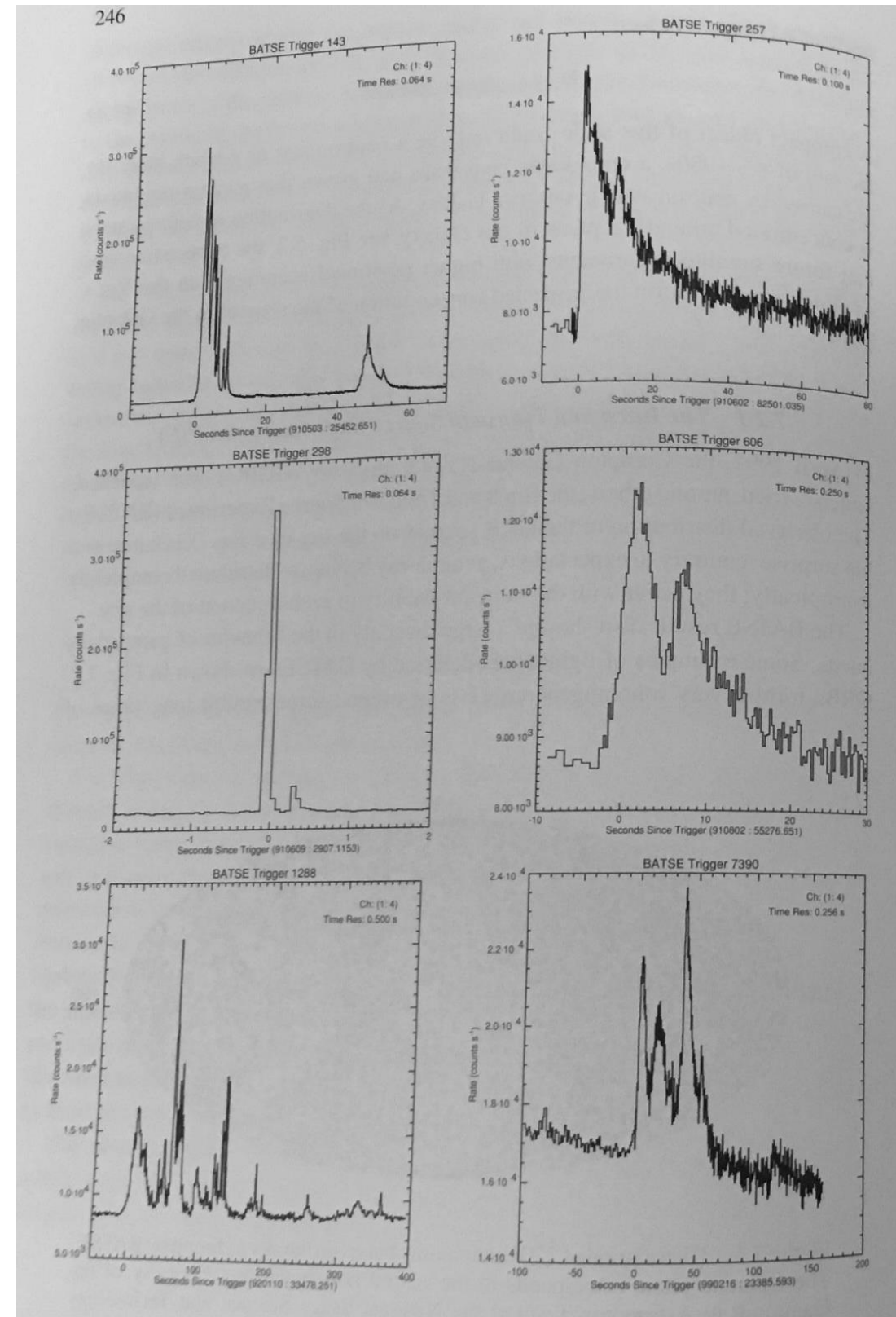
Galactic
MW halo
Extragalactic

BATSE sky distribution

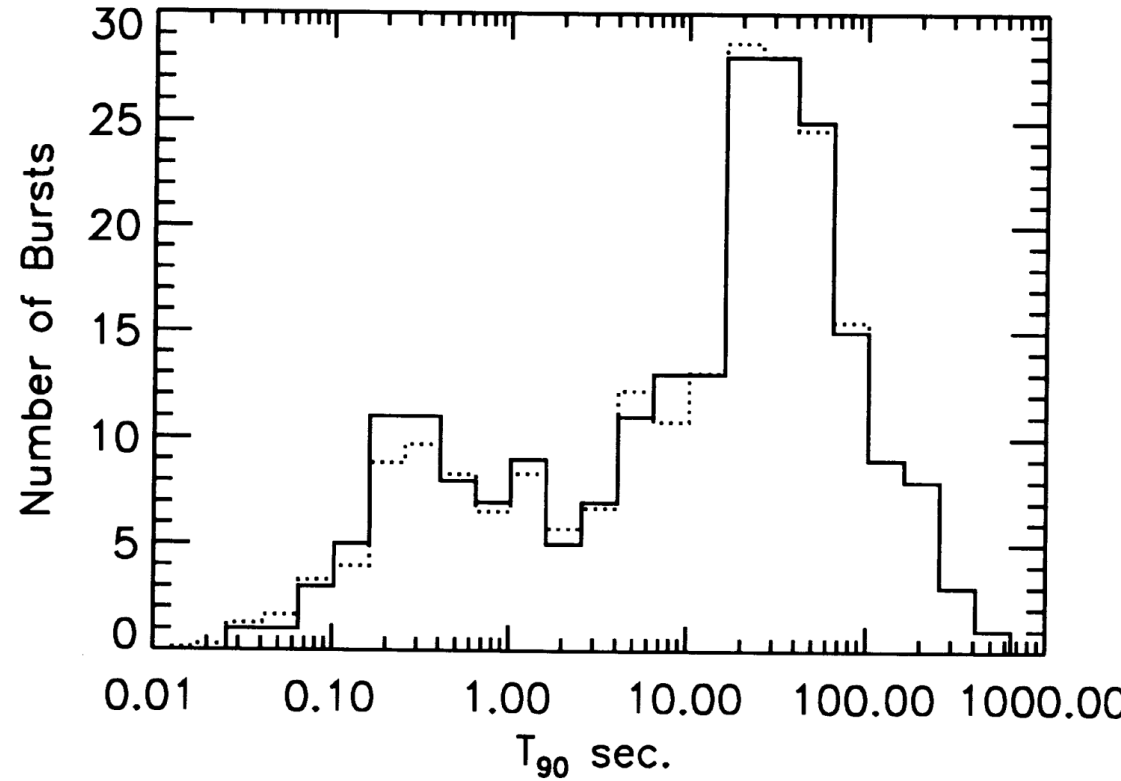
2704 BATSE Gamma-Ray Bursts



BATSE time series



Identification of two classes of gamma-ray bursts



5. DISCUSSION

We have linked here for the first time the duration bimodality with the hardness-duration correlation of GRBs. Previous studies have reported evidence for either the former (Cline & Desai 1974; Mazets et al. 1981; Klebesadel 1990; Norris et al. 1984; Hurley 1991) or the latter (Dezalay et al. 1991). Our study shows that the two classes separated by duration are also associated with significantly different average hardness ratios. We find that the short events have the same peak intensity range as the longer ones; this makes the total amount of energy released by the two types significantly different. Both short and long GRBs have isotropic but inhomogeneous spatial distributions. All evidence suggests that both GRB subsets originate from the same type of objects. Different geometries of their emission sites (with respect to the observer) may be responsible for the spectral and temporal differences between the classes.

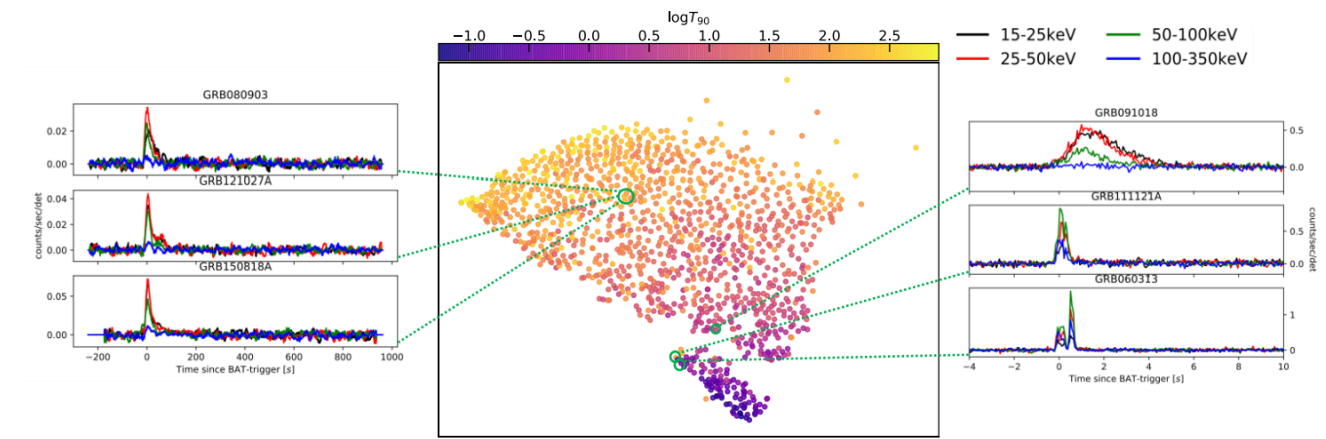


Figure 1. t-SNE mapping of *Swift* light curves, colored based on duration $\log(T_{90})$. Several sample light curves in the four observed bands are shown, with similar light curves placed as near neighbours and dissimilar light curves placed further apart. A clear separation into two groups is visible, with the smaller, bottom group (referred to as type-S) generally but not uniformly of shorter duration (see Fig. 2). The axes resulting from t-SNE have no clear physical interpretation or units; only the structure is meaningful.

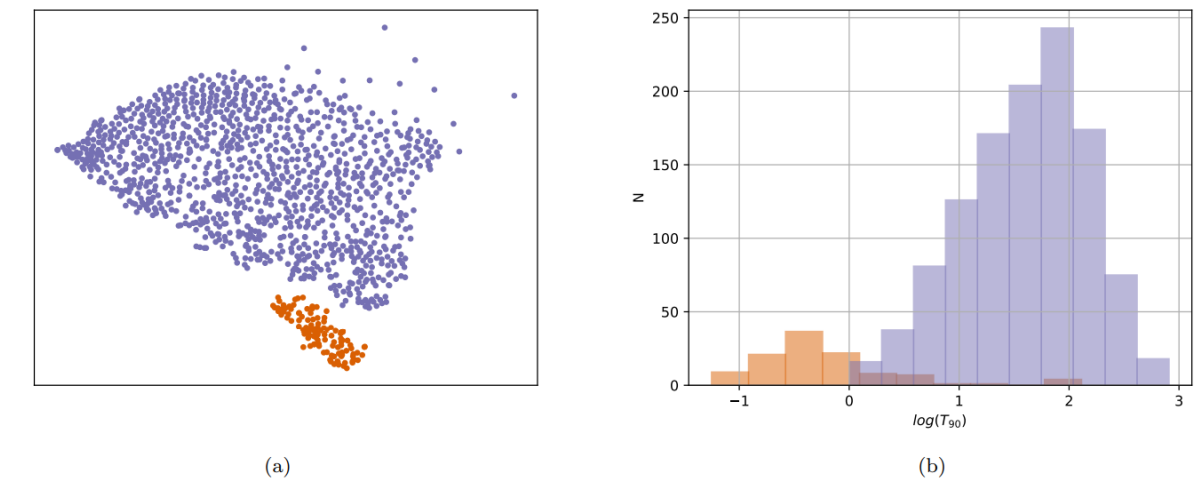


Figure 2. (a) The clear separation into two groups (purple and orange) strongly suggests a classification of GRBs into two distinct types. (b) The distributions of duration in $\log(T_{90})$ of type-L and type-S bursts are approximately normal and similar to those expected for a long- and short classification.

Afterglow identification: long GRBs

Table 2.1. Comparison of directional gamma-ray burst experiments

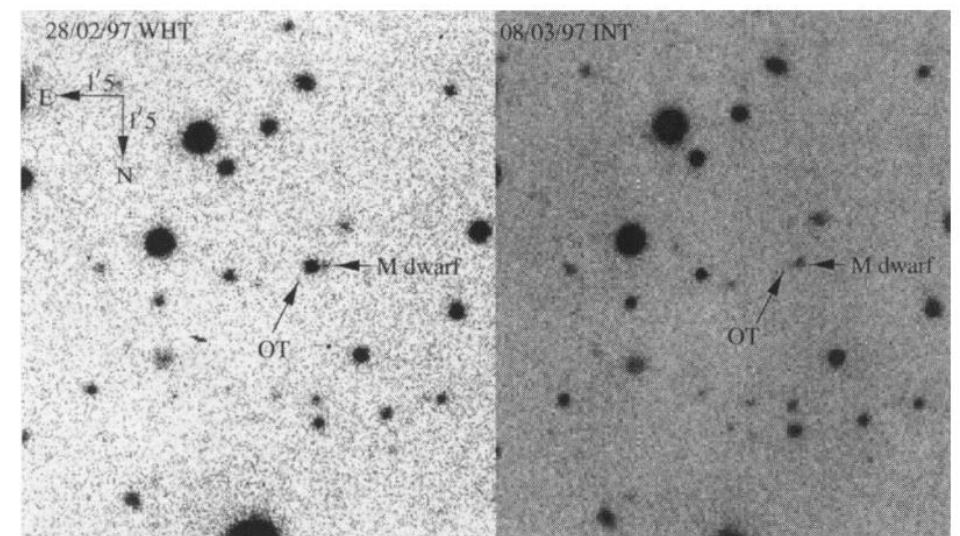
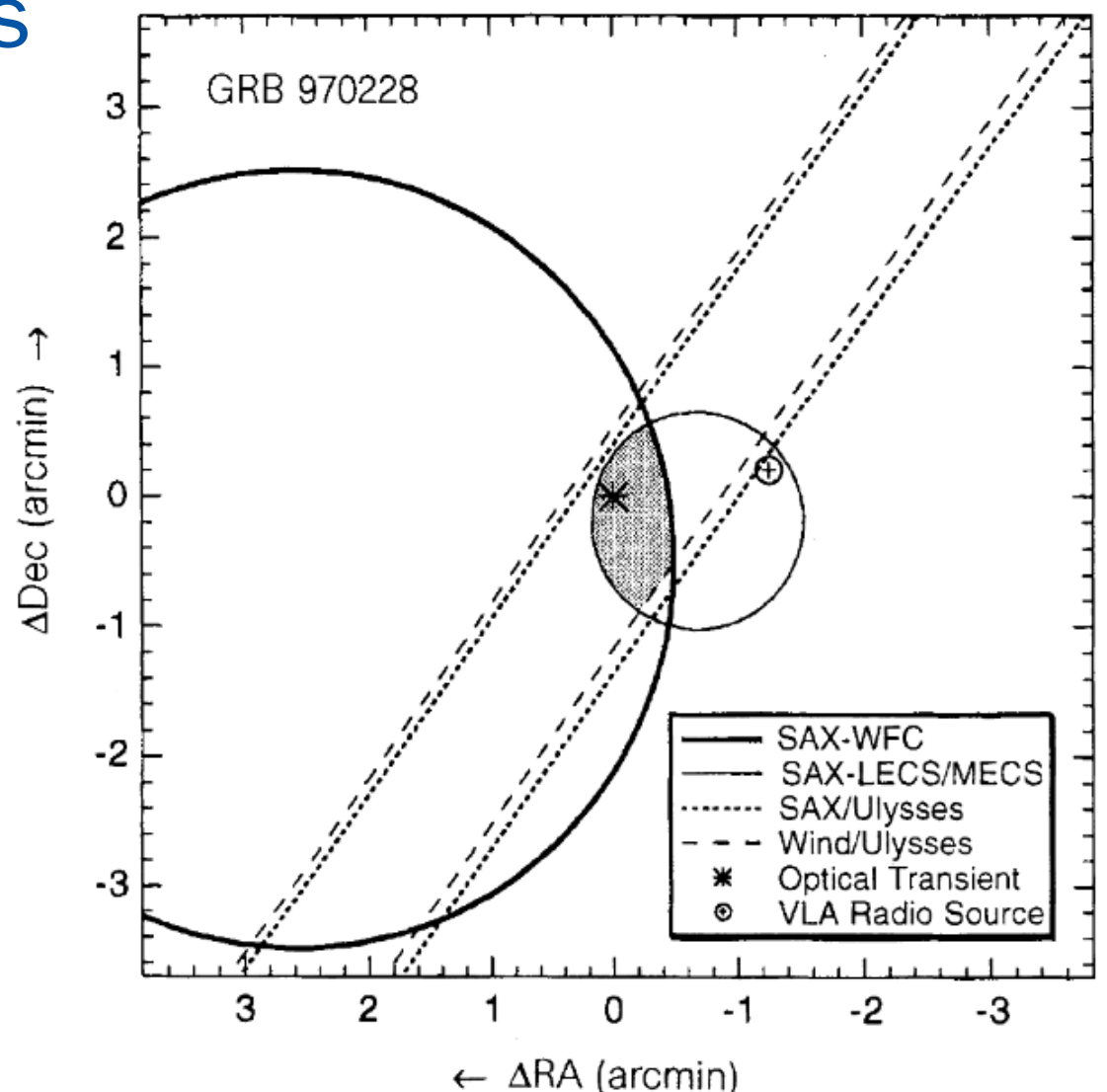
	Strategy	FoV ^a	$\Delta\theta^b$	#/yr	ΔT^c
<i>Vela</i>	multiple Earth satellites	12.5	50°	5	days
<i>IPN</i>	multiple Solar System satellites	12.5	2'	15	12 hr
BATSE	8 cosine-law detectors	7.5	3°	300	1.5 hr
COMPTEL	Compton telescope	1	1°	5	7 min
<i>BeppoSAX</i>	gamma-ray coded aperture, X-ray telescope, ground processing for location	0.6	3'	10	5 hr
<i>HETE-WXM</i>	X-ray coded aperture, gamma-ray detector, on-board positioning, always real-time telemetry to ground	1.5	10'	30	50 s
<i>HETE-SXC</i>	soft X-ray coded aperture, on-board positioning	1	30''	15	50 s
<i>Swift-BAT</i>	gamma-ray coded aperture, onboard positioning, self-tasking satellite	1.4	2'	100	70 s
<i>Swift-NFI</i>	UV, X-ray telescopes, on-board positioning, self-tasking satellite	1.4	1–3''	100	70 s
<i>Fermi/GBM</i>	12 cosine-law detectors, electron-pair tracker	9	8°	240	10 s

^a steradians

^b accuracy of GRB position

^c time to achieve GRB position

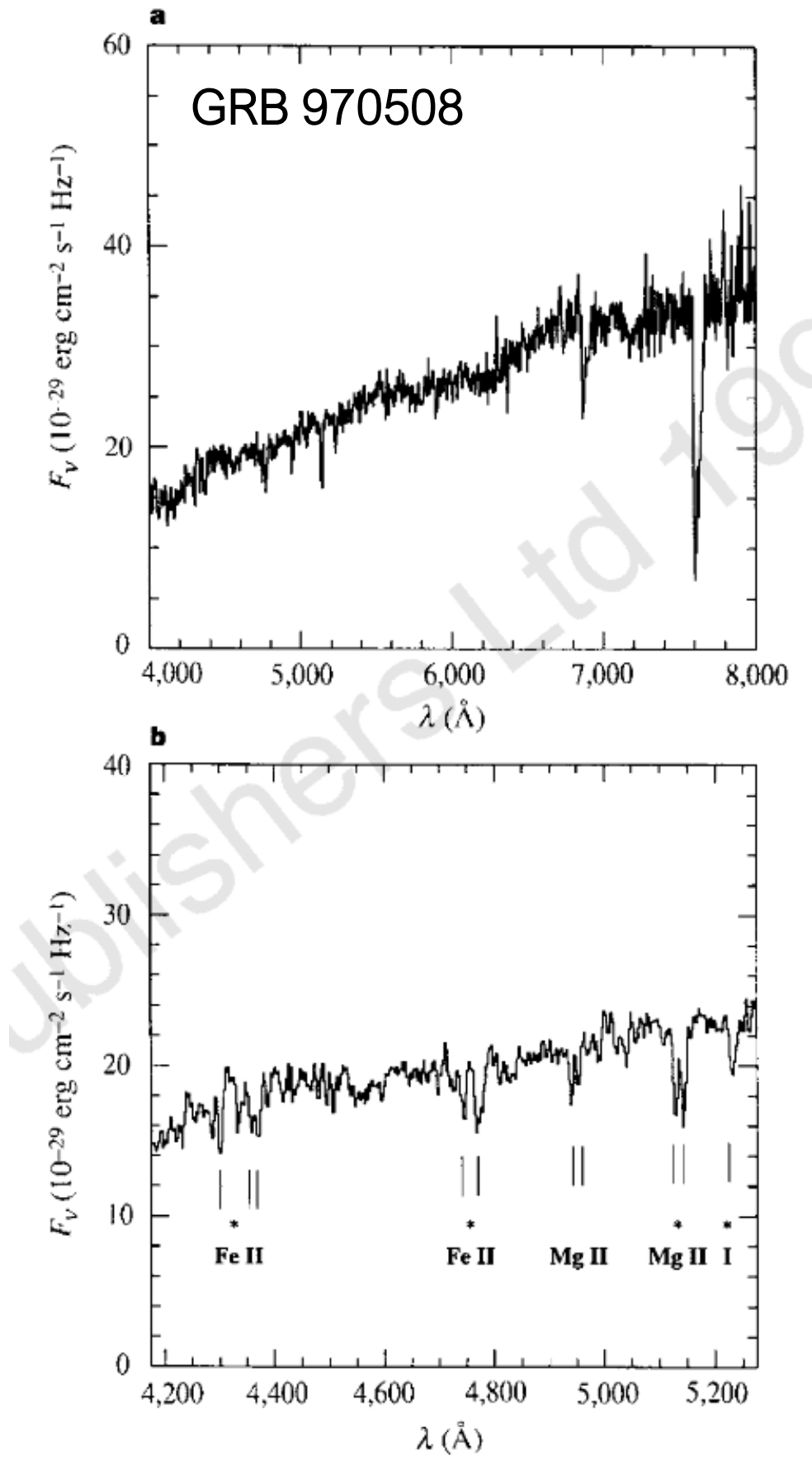
For almost a quarter of a century¹, the origin of γ -ray bursts—brief, energetic bursts of high-energy photons—has remained unknown. The detection of a counterpart at another wavelength has long been thought to be a key to understanding the nature of these bursts (see, for example, ref. 2), but intensive searches have not revealed such a counterpart. The distribution and properties of the bursts³ are explained naturally if they lie at cosmological distances (a few Gpc)⁴, but there is a countervailing view that they are relatively local objects⁵, perhaps distributed in a very large halo around our Galaxy. Here we report the detection of a transient and fading optical source in the error box associated with the burst GRB970228, less than 21 hours after the burst^{6,7}. The optical transient appears to be associated with a faint galaxy^{7,8}, suggesting that the burst occurred in that galaxy and thus that γ -ray bursts in general lie at cosmological distance.



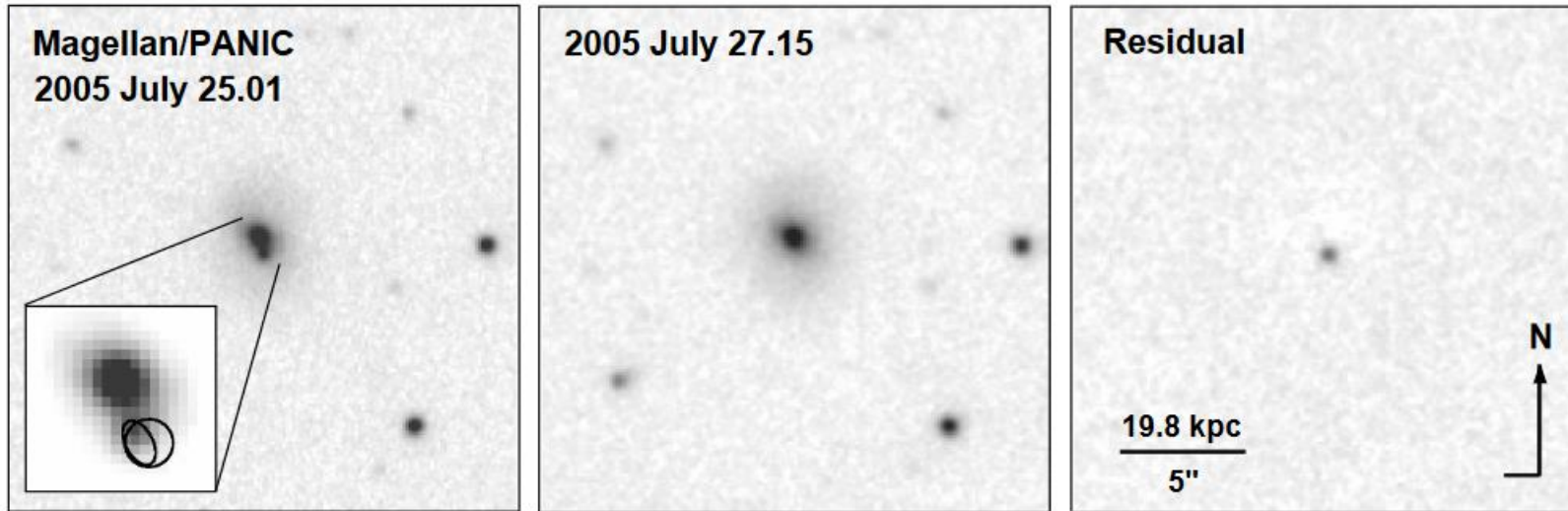
Afterglow identification: long GRBs

First measured afterglow
redshift at $0.835 \leq z \leq 2.3$
confirmed extragalactic origin
and set energy scale

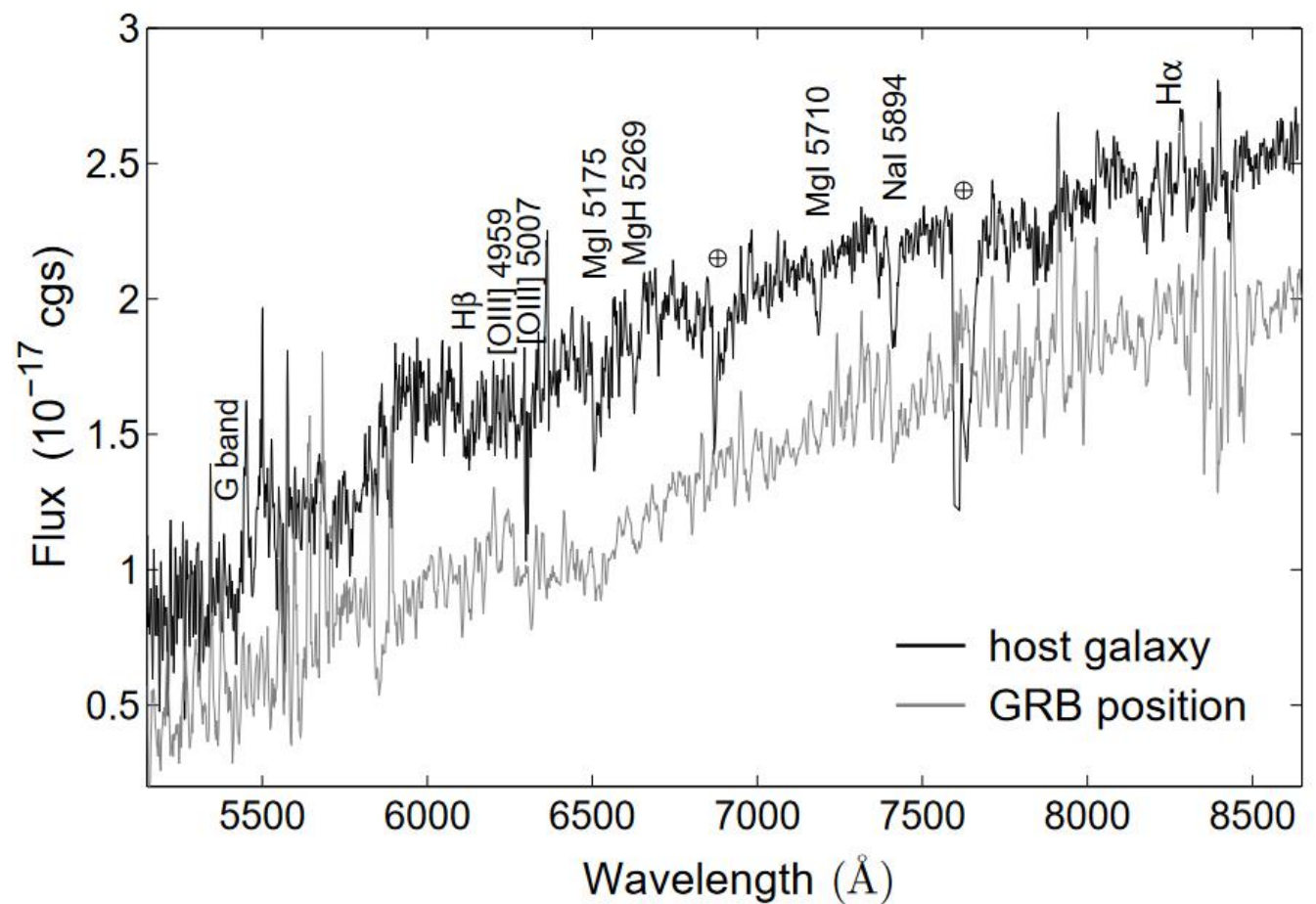
The remarkable progress in detecting X-ray and optical counterparts to GRBs has been made possible only by rapid localization of the burst by BeppoSAX and prompt dissemination of the coordinates by the BeppoSAX team. Further progress in understanding GRBs requires many more optical counterparts to be identified. It is clear from experience of the first two optical counterparts that, in order to obtain the critical data, the counterparts must be discovered and followed up spectroscopically within a few days. It now seems that an understanding of the physical mechanisms behind γ -ray bursts is within reach.



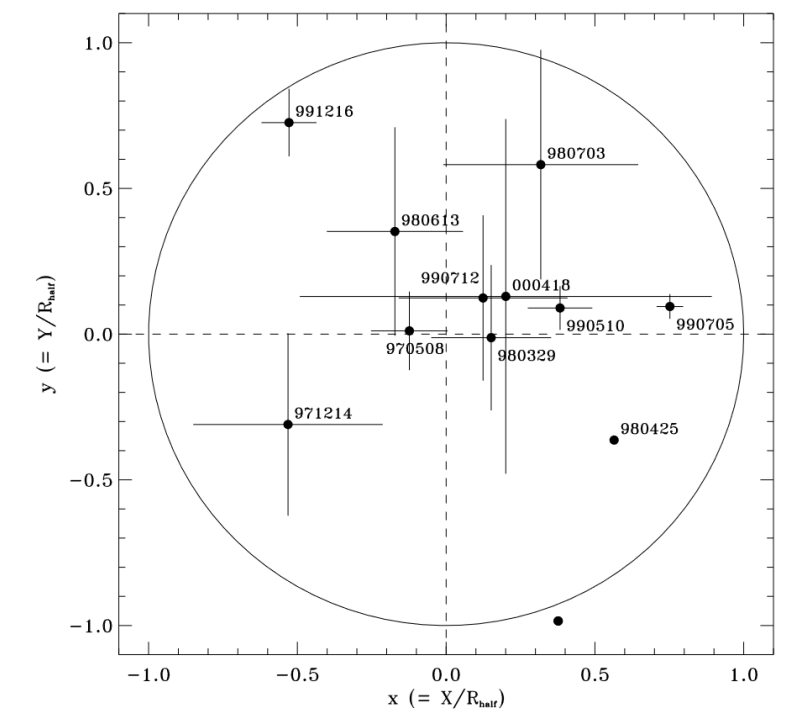
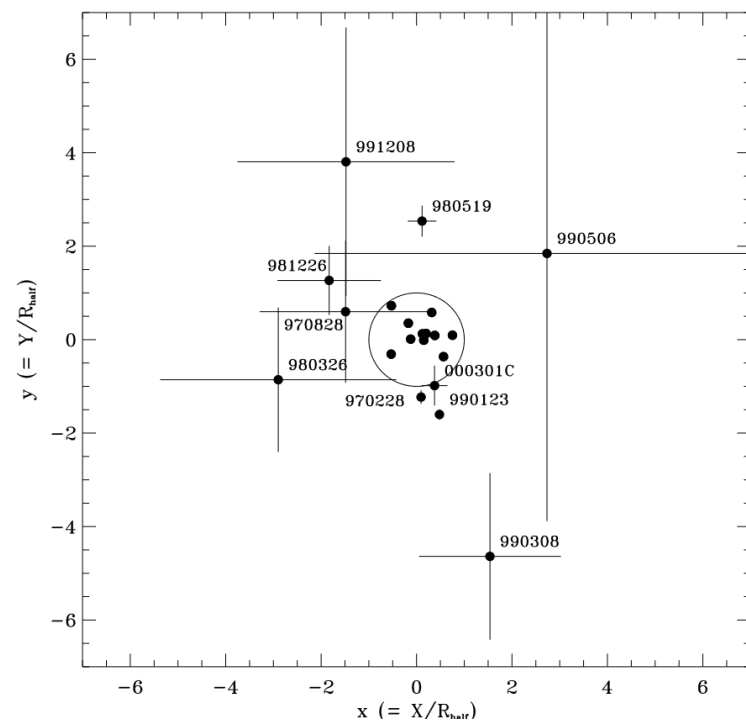
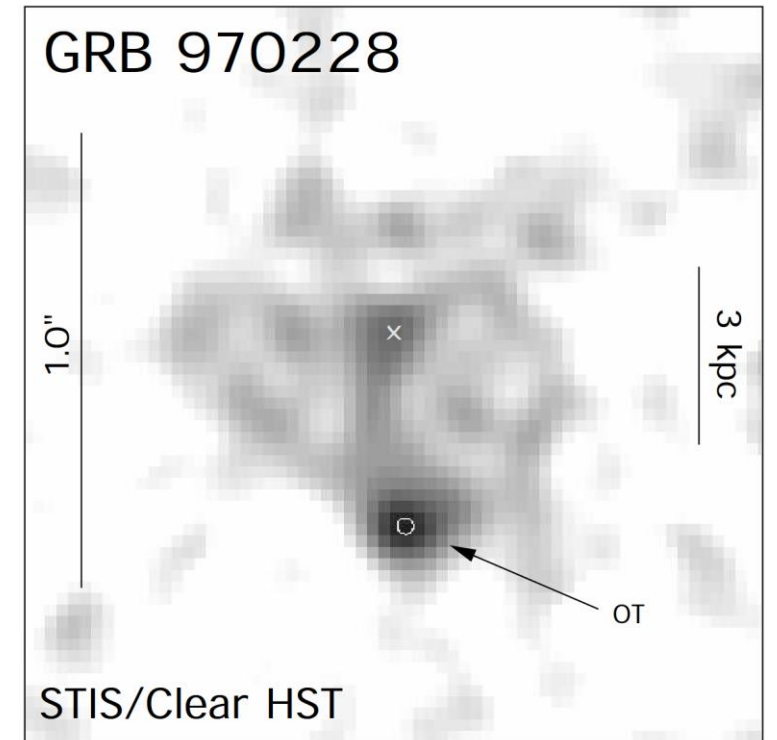
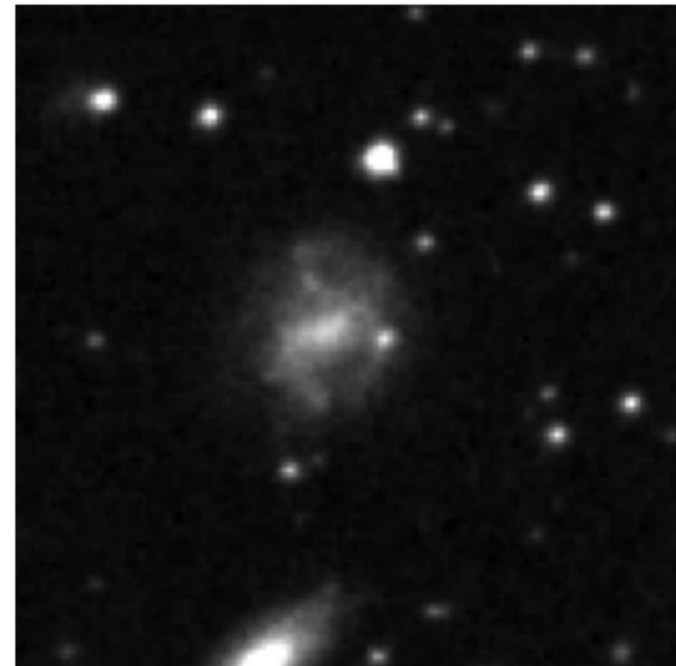
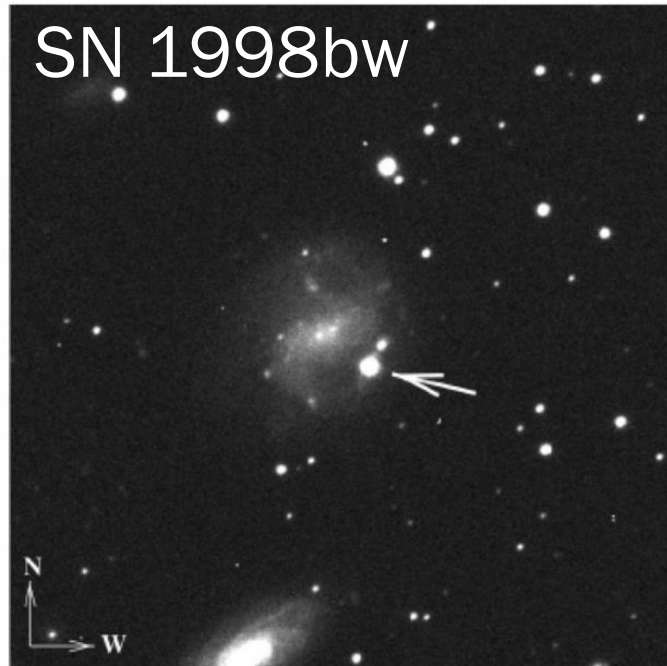
Afterglow identification: short GRBs



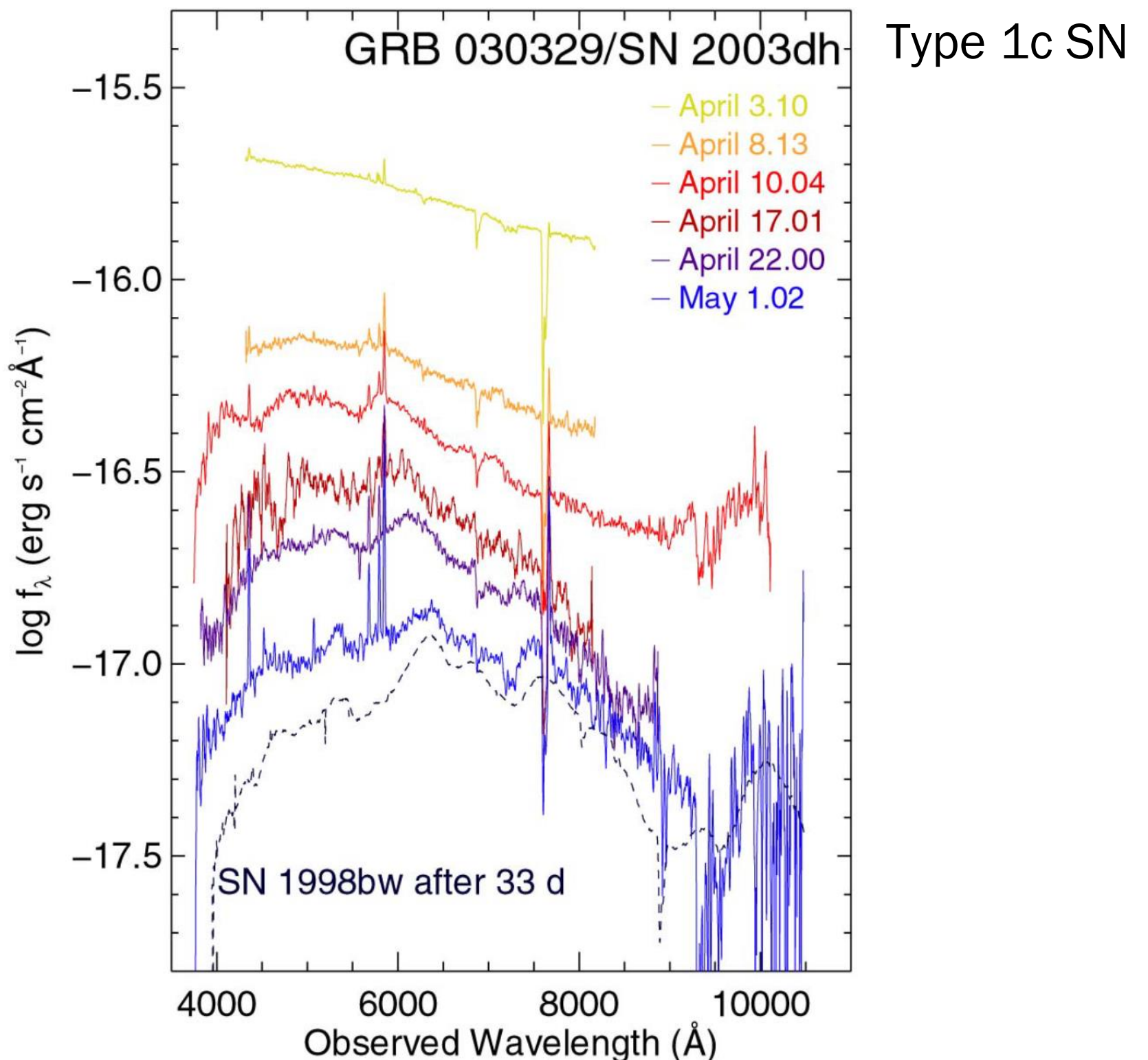
First measured afterglow
redshift at $z = 0.257 \pm 0.001$
confirmed extragalactic origin
and set energy scale



Supernova connection: long GRBs



Supernova connection: long GRBs



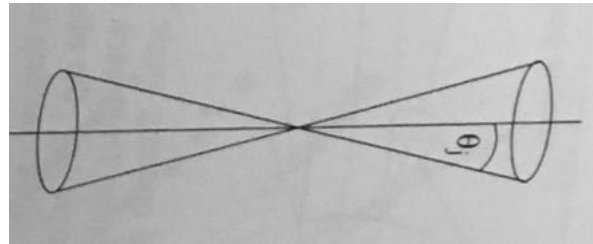
Long vs. short GRBs

261

Table 7.2 Comparison of the properties of long and short GRBs.

Property	Long GRB	Short GRB
Duration	~30 s	~0.3 s
Observed rate (BATSE)	~500 yr ⁻¹	~170 yr ⁻¹
Variability timescale	~1 ms	~1 ms
Host galaxy	Galaxies with active star formation	Galaxies with and without star formation
Supernova?	Confirmed in some cases	Prob. not
Isotropized γ -energy $E_{\gamma,\text{iso}}$	$\sim 10^{53}$ erg	$\sim 10^{50}$ erg
Median redshift	~2	~0.3
Popular model	“collapsar”	Compact binaries

Beaming



$$E_{\text{true}} = E_{\text{iso}} \left(\frac{\Delta\Omega}{4\pi} \right).$$

$$E_{\text{true}} \approx E_{\text{iso}} \left(\frac{\theta_j^2}{2} \right) \approx \frac{E_{\text{iso}}}{65} \left(\frac{\theta_j}{10^\circ} \right)^2.$$

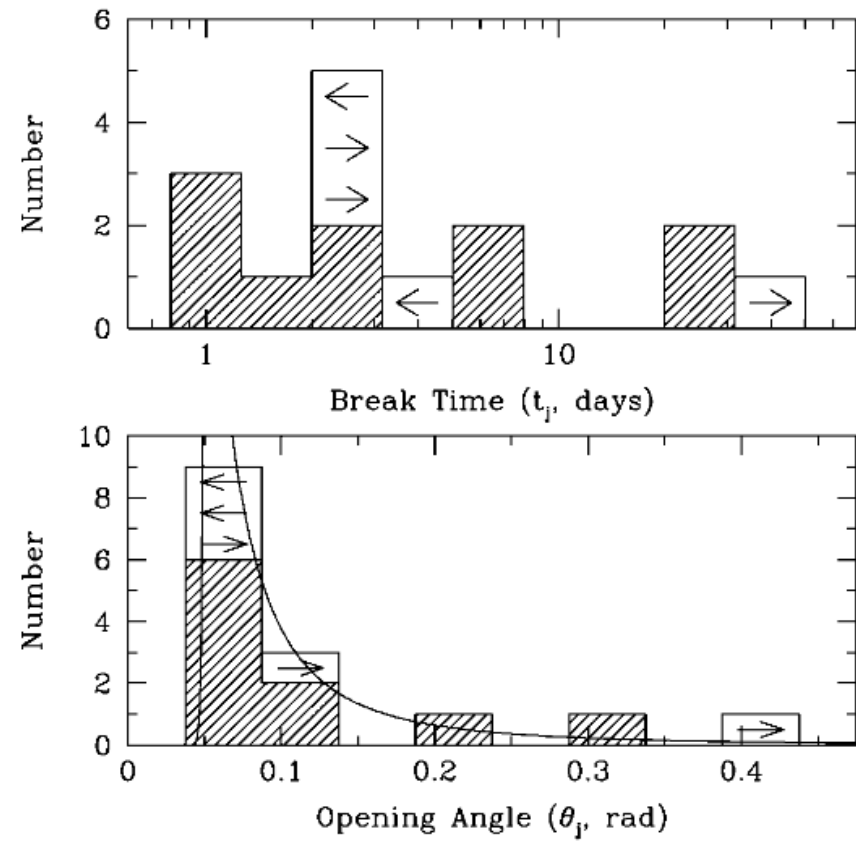


FIG. 1.—Observed distribution of jet break times (top panel) and jet opening angles (bottom panel). For the model fit (solid line), we assume that the observed differential distribution of beaming factors can be represented by two power laws: $p_{\text{obs}}(f_b) = (f_b/f_0)^{\alpha+1}$ for $f_b < f_0$ and $p_{\text{obs}}(f_b) = (f_b/f_0)^{\beta+1}$ for $f_b > f_0$. Since for every observed burst there are f_b^{-1} that are not observed, the true distribution is $p_{\text{true}}(f_b) = f_b^{-1} p_{\text{obs}}(f_b)$. Fitting to the data, we find the following: α is poorly constrained; $\beta = -2.77^{+0.24}_{-0.30}$; and $\log f_0 = -2.91^{+0.07}_{-0.06}$. Thus, the true differential probability distribution (under the small angle approximation, $f_b \propto \theta_j^2$) is given by $p_{\text{true}}(\theta_j) \propto \theta_j^{-4.54}$ with the observed distribution being $p_{\text{obs}} \propto \theta_j^{-2.54}$. The distribution $p_{\text{true}}(f_b)$ allows us to estimate the true correction factor, $\langle f_b^{-1} \rangle$ that has to be applied to the observed GRB rate in order to obtain the true GRB rate. We find $\langle f_b^{-1} \rangle = f_0^{-1}[(\beta - 1)/\beta] \sim 520 \pm 85$.

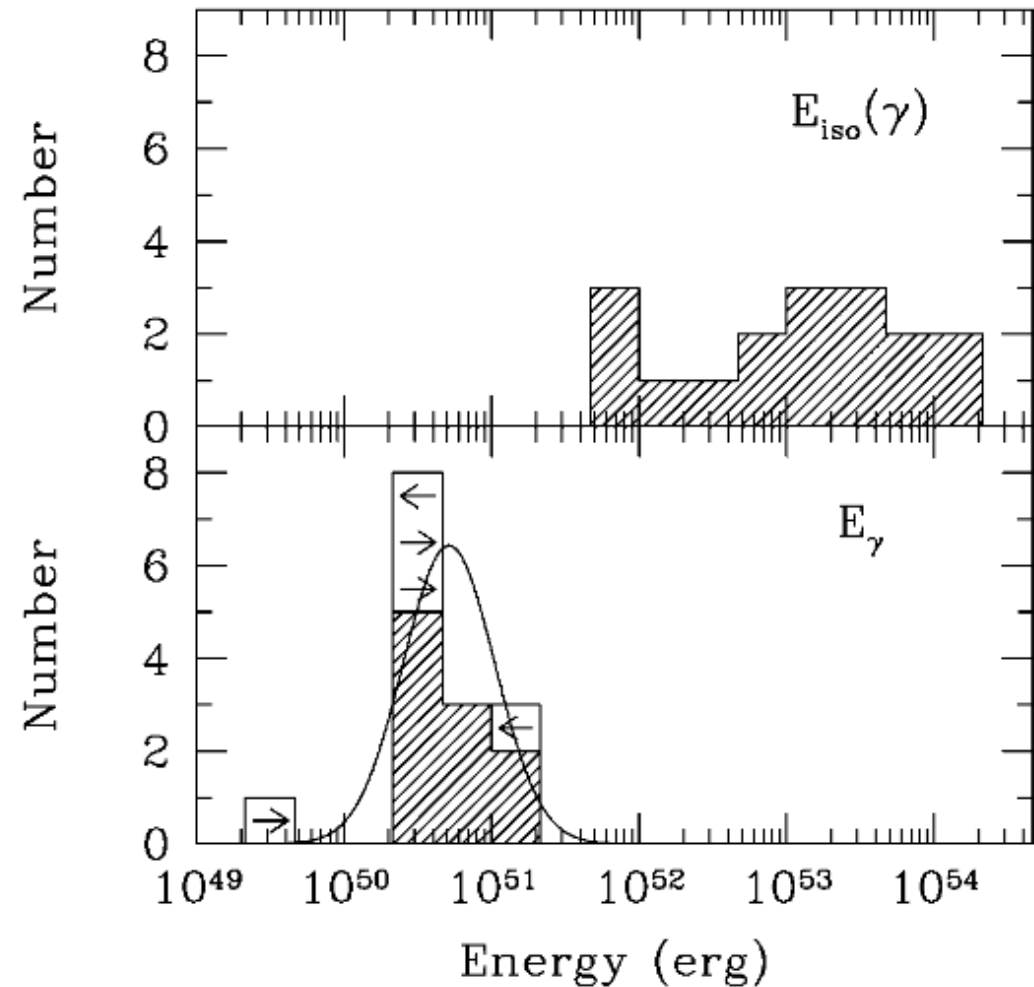


FIG. 2.—Distribution of the apparent isotropic GRB energy of GRBs with known redshifts (top panel) vs. the geometry-corrected energy for those GRBs whose afterglows exhibit the signature of a nonisotropic outflow (bottom panel). Arrows are plotted for five GRBs to indicate upper or lower limits to the geometry-corrected energy.

Compactness problem and relativistic resolution

$$E = 4\pi b^2 F = 10^{50} \text{ ergs} \left(\frac{D}{3000 \text{ Mpc}} \right)^2 \left(\frac{F}{10^{-7} \text{ ergs/cm}^2} \right)$$

10 ms variability $\Rightarrow R < c\Delta t \approx 3000 \text{ km}$

high-energy photons $\Rightarrow \gamma\gamma \rightarrow e^+e^-$
 if $\sqrt{E_1 E_2} > m_e c^2$ let's say true for
 fraction f_p

$$\tau_{\gamma\gamma} = \frac{f_p \sigma_T F D^2}{R^2 m_e c^2} = 10^{13} f_p \left(\frac{F}{10^{-7} \text{ ergs/cm}^2} \right) \left(\frac{D}{3000 \text{ Mpc}} \right) \left(\frac{\Delta t}{10 \text{ ms}} \right)^{-2}$$

Relativistic:

or

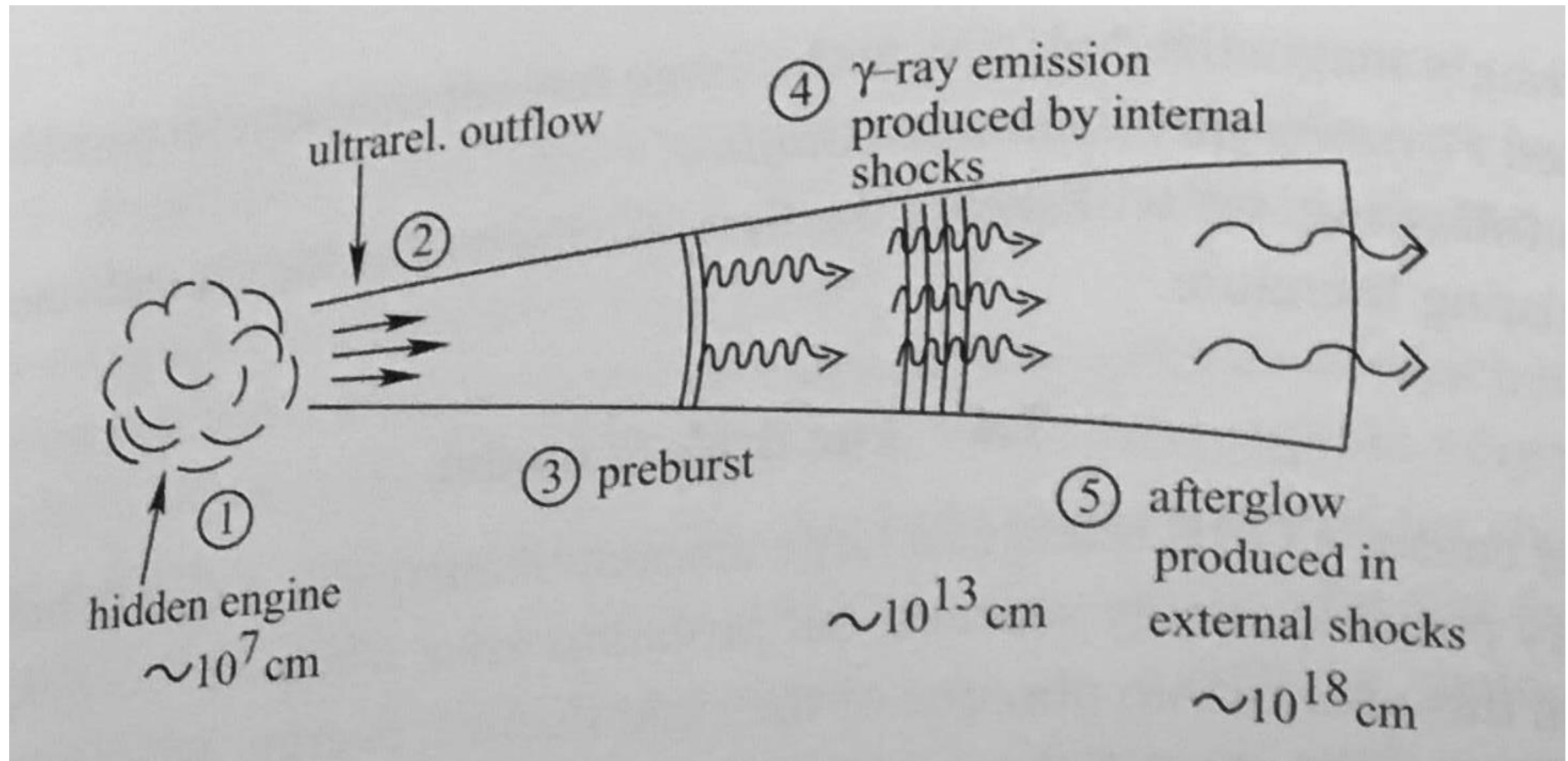
$$\tau_{\gamma\gamma} = \frac{f_p}{\gamma^{2\alpha}} \frac{\sigma_T F D^2}{R^2 m_e c^2},$$

$$\tau_{\gamma\gamma} \approx \frac{10^{13}}{\gamma^{(4+2\alpha)}} f_p \left(\frac{F}{10^{-7} \text{ ergs/cm}^2} \right) \left(\frac{D}{3000 \text{ Mpc}} \right)^2 \left(\frac{\delta T}{10 \text{ msec}} \right)^{-2}$$

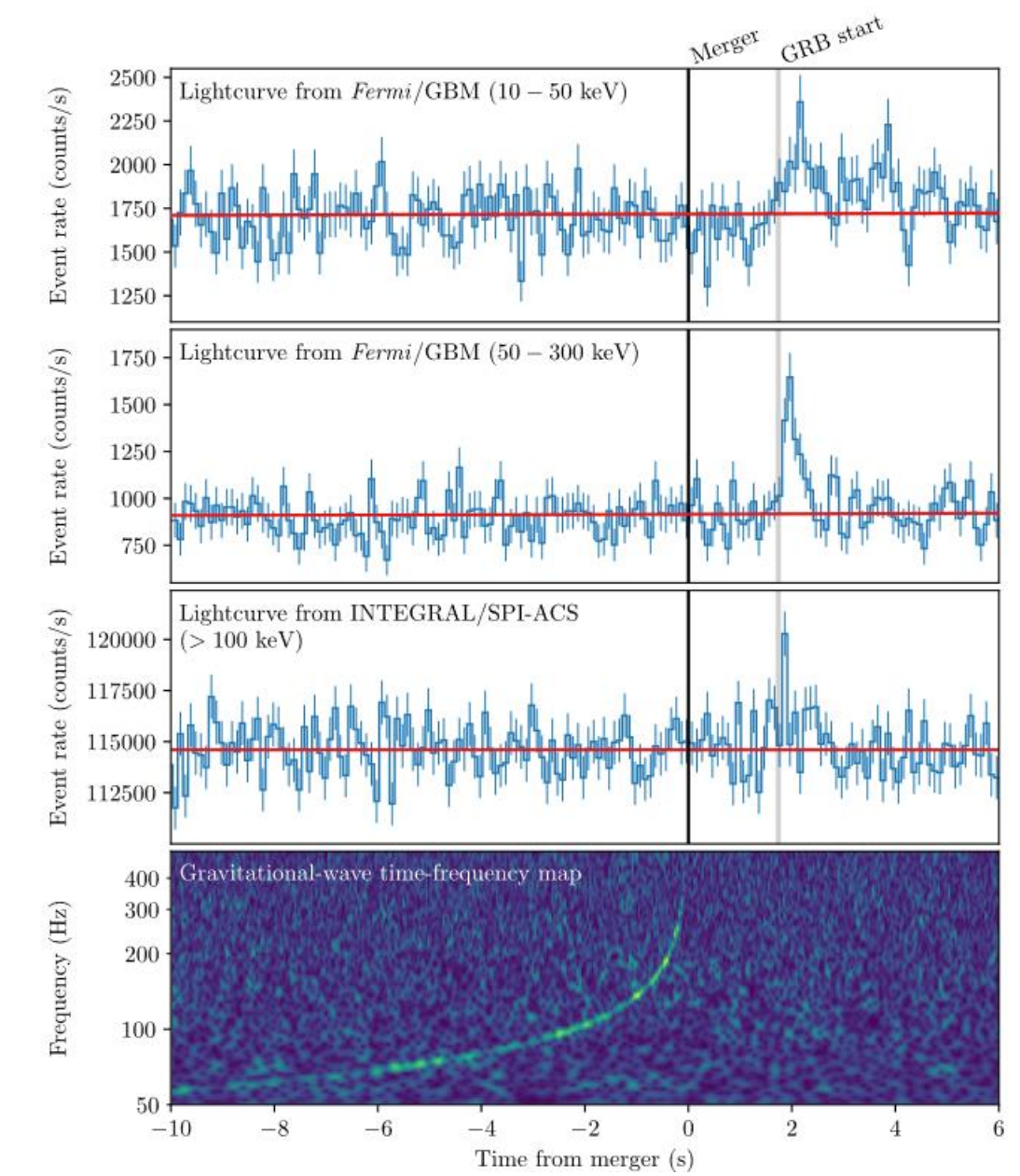
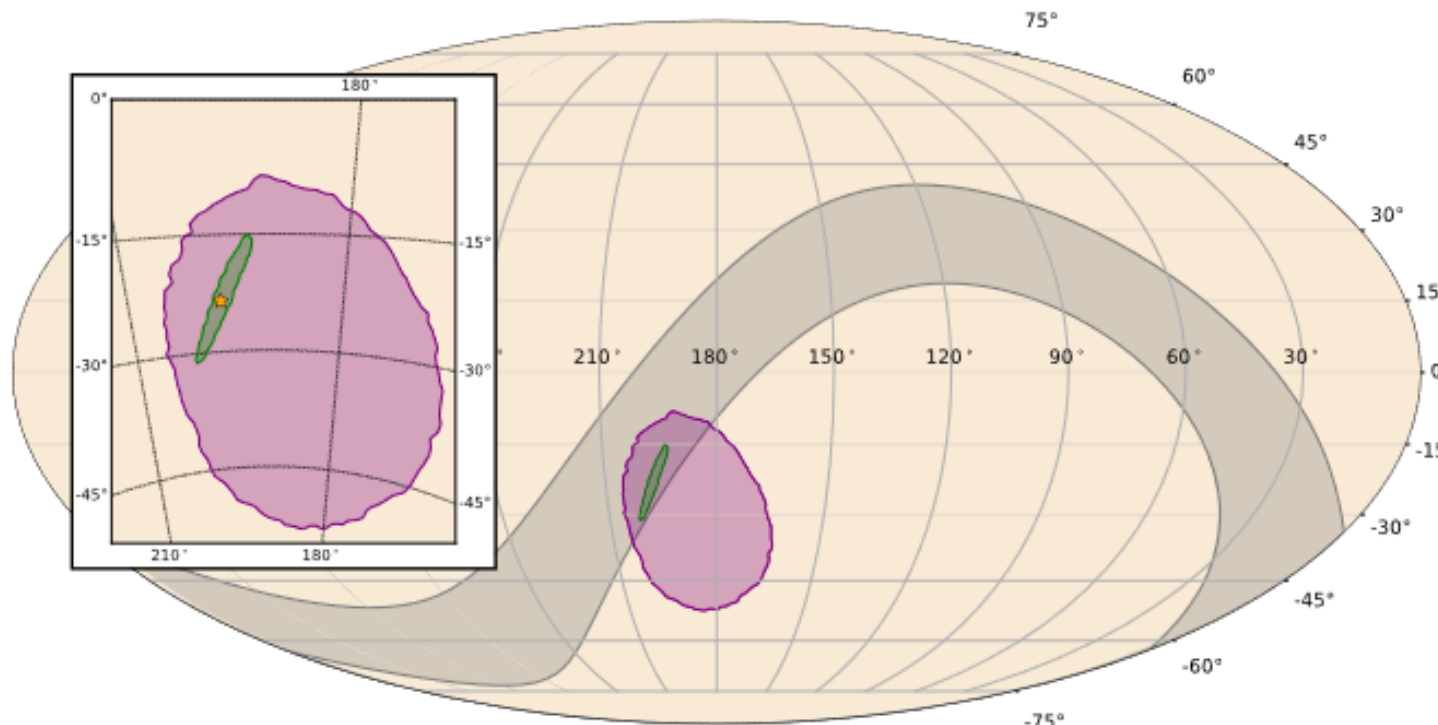
(10)

Baryonic pollution problem

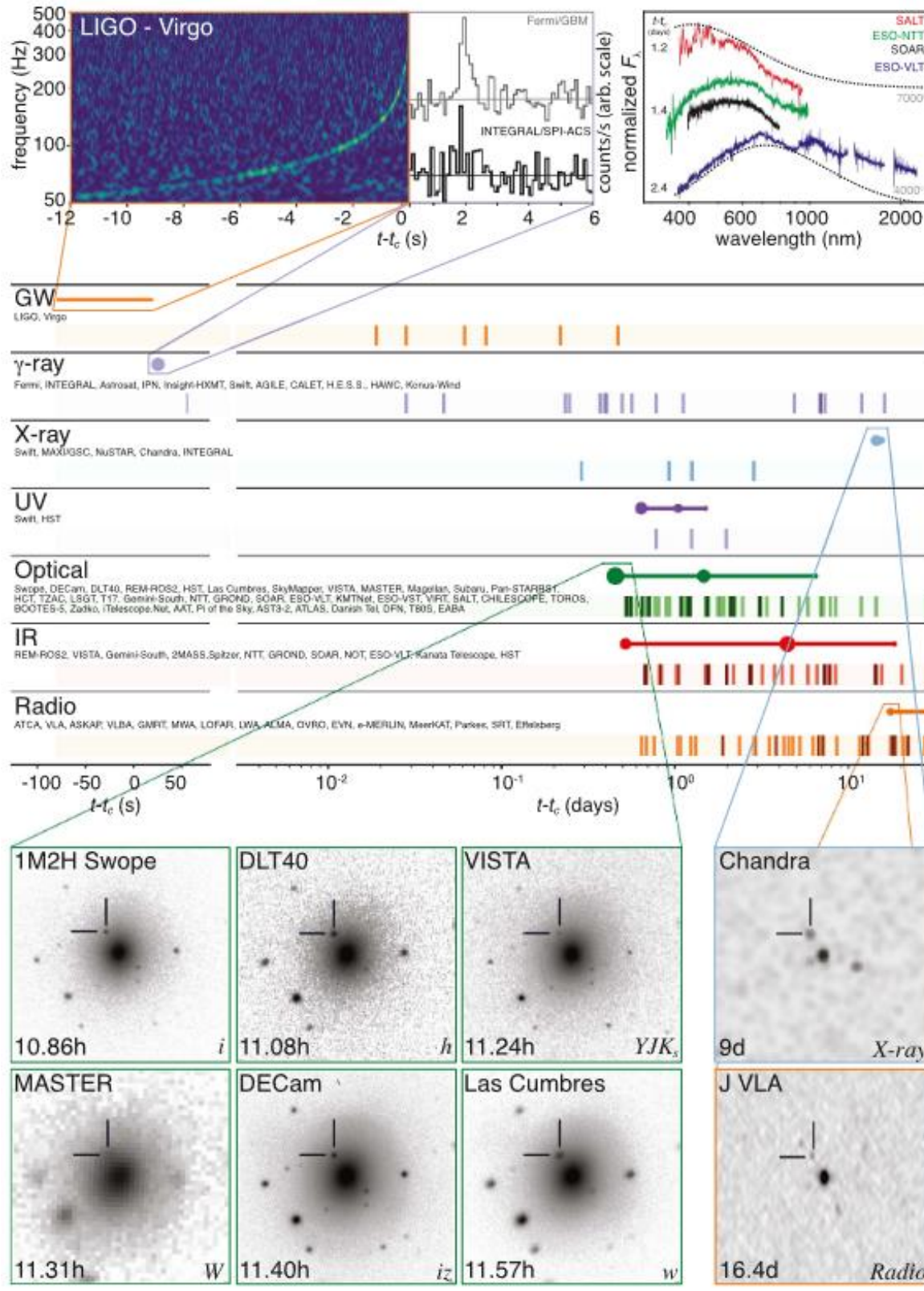
Fireball model



GW170817

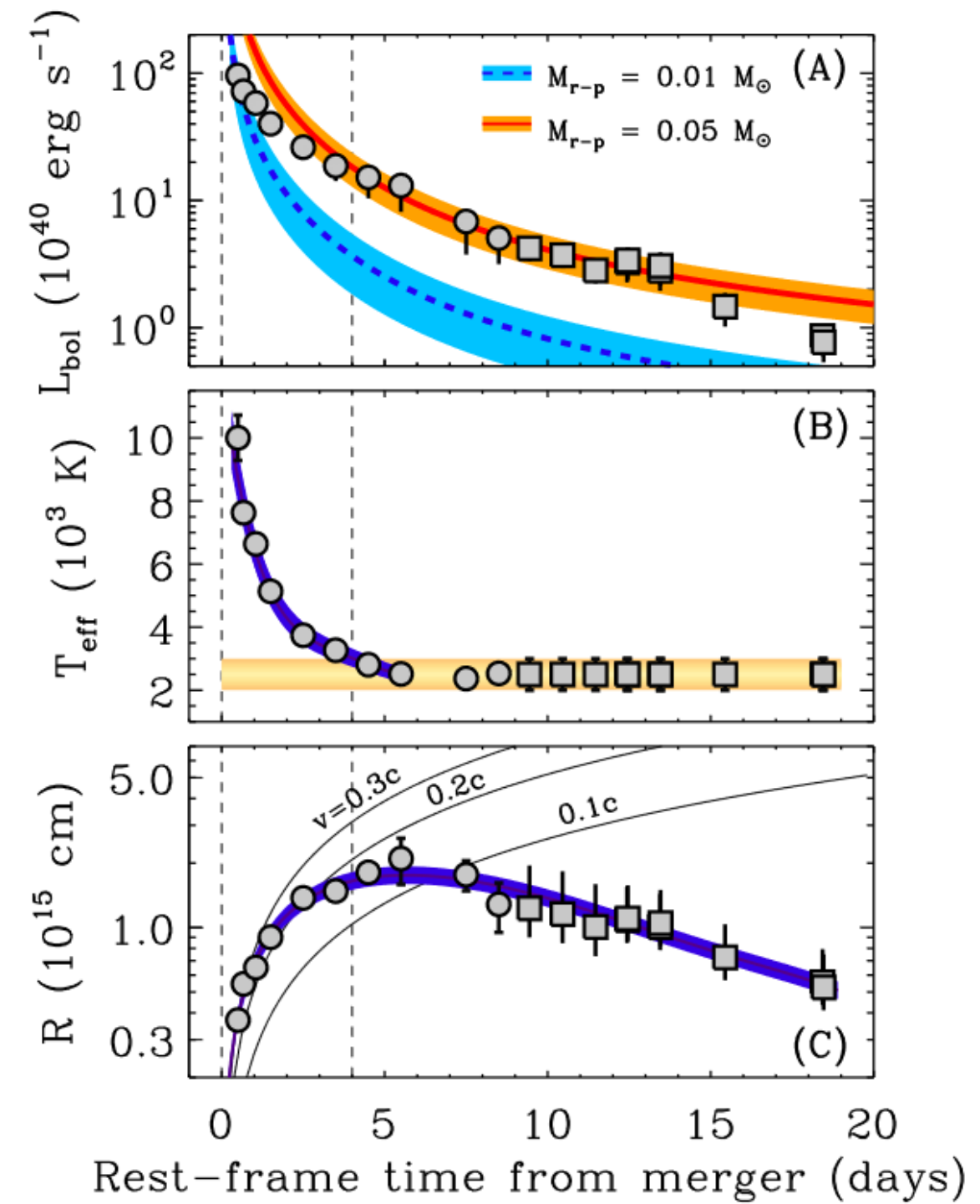
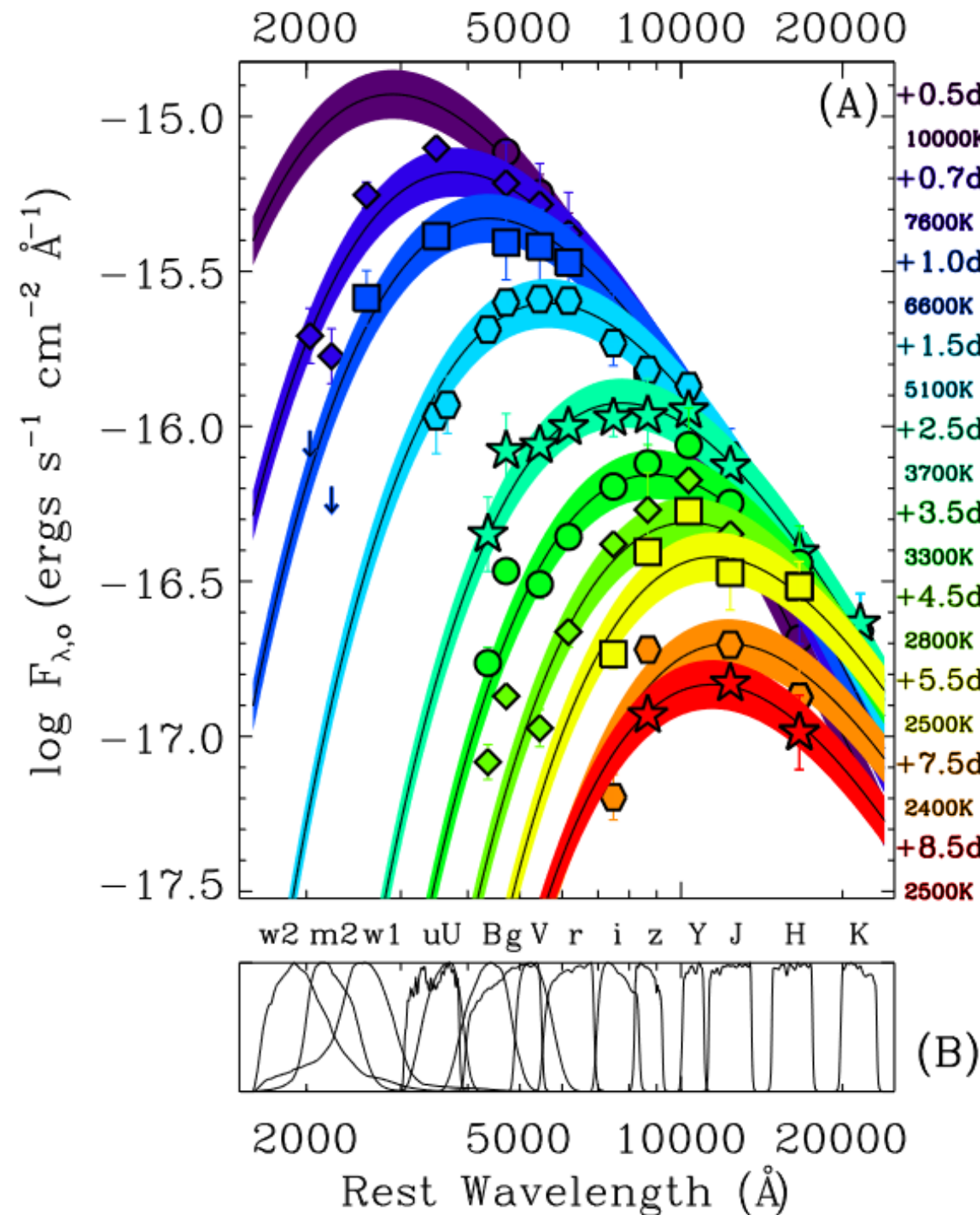


GW170817



GW170817

Need r-process
radioactive heating



GW170817

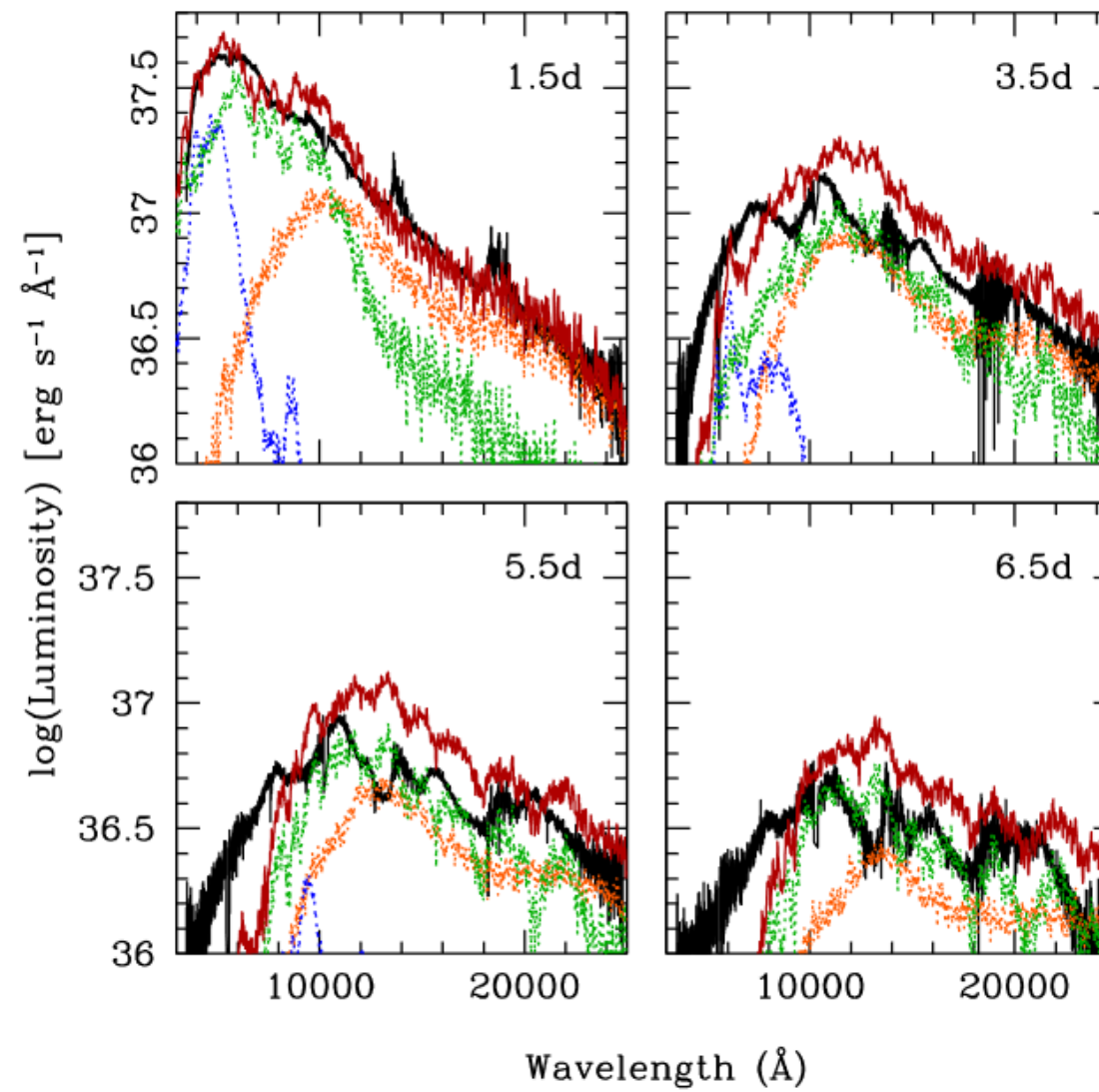


Figure 3: Kilonova model compared to the AT 2017gfo spectra. X-shooter spectra (black line) at the first four epochs and kilonova models: dynamical ejecta ($Y_e = 0.1 - 0.4$, orange), wind region with proton fraction $Y_e = 0.3$ (blue) and $Y_e = 0.25$ (green). The red curve represents the sum of the three model components.